South African Journal of Chemical Engineering 43 (2023) 348–358

Contents lists available at ScienceDirect

South African Journal of Chemical Engineering

journal homepage: www.elsevier.com/locate/sajce

Co-pyrolysis of oil palm trunk and polypropylene: Pyrolysis oil composition and formation mechanism

Liza Melia Terry [a], Melvin Xin Jie Wee [b], Jiuan Jing Chew [a], Deni Shidqi Khaerudini [c], Gerald Ensang Timuda [c], Aqsha Aqsha [d], Agus Saptoro [b], Jaka Sunarso [a,*]

[a] Research Centre for Sustainable Technologies, Faculty of Engineering, Computing and Science, Swinburne University of Technology, Jalan Simpang Tiga, Kuching, Sarawak, 93350, Malaysia
[b] Department of Chemical and Energy Engineering, Curtin University Malaysia, CDT 250, Miri, Sarawak, 98009, Malaysia
[c] Research Center for Advanced Materials, National Research and Innovation Agency (BRIN), Bld. 440 Kawasan Puspiptek Serpong, South Tangerang Banten, 15314, Indonesia
[d] Department of Bioenergy Engineering and Chemurgy, Faculty of Industrial Technology, Institut Teknologi Bandung, Bandung, Jawa Barat, 40132, Indonesia

ARTICLE INFO

Keywords:
Co-pyrolysis
Mechanism
Oil palm trunk
Plastics
Polypropylene
Pyrolysis oil

ABSTRACT

Pyrolysis oil can be used as a precursor to synthesize value-added biochemicals. Co-pyrolysis of two or more feedstocks generally improves the selectivity and yield of the target compounds. In this work, oil palm trunk (OPT) was subjected to single-feed pyrolysis and co-pyrolysis with polypropylene (PP) from 500 to 700 °C. The highest pyrolysis oil yield of 26.33 wt.% was obtained from OPT at 700 °C, which mainly contributed by the lignin decomposition in OPT. Phenolics (51.77–57.78%) and oxygenates (36.31–46.99%) were the major compounds detected in the OPT-derived pyrolysis oil. The addition of PP enhanced the formation of hydrocarbons (5.19–10.22%) and decreased the contents of phenolics (34.01–41.85%) in the co-pyrolysis oil. In the case of co-pyrolysis, the intermolecular reactions between PP and OPT-derived radicals led to the formation of ketones and alcohols, which contributed to the increase of oxygenates content. The highest oil yield of 16.17 wt.% was obtained at 600 °C from co-pyrolysis, the oil of which contained mainly phenolic compounds, oxygenated compounds (i.e., ketones and furans), and hydrocarbons. These findings highlighted the potential of oil derived from the pyrolysis of OPT (single feed) and co-pyrolysis of OPT and PP (binary feed) for the production of value-added chemicals.

1. Introduction

The depletion of non-renewable fossil fuels triggers the global energy crisis due to high energy demand. At the same time, this motivates the development of renewable alternatives (i.e., biomass, solar, hydroelectric energy, and etc.) to resolve this issue. Pyrolysis oil is a sustainable alternative to fossil fuels since it can be produced from renewable resources such as lignocellulosic biomass *via* pyrolysis (Chan et al., 2019). Pyrolysis is generally a more attractive route since it allows the use of different feedstock and operating conditions. Pyrolysis can be operated at a wide temperature range of 300 to 900 °C under atmospheric pressure (Yaman, 2004; Zhang et al., 2016). The rich composition of pyrolysis oil with more than 300 chemical constituents enables its use as the precursor for the synthesis of value-added chemicals (Machado et al., 2022).

As the second largest palm oil producer in the world, Malaysia produced about 310 million tons of oil palm biomass waste from the oil palm industry in 2021 alone. These biomasses can be harnessed as feedstock for pyrolysis oil production. Table S1 in **Supplementary Information** provides the approximate amounts of various types of oil palm biomass generated per weight of fresh fruit bunch or hectare of oil palm plantation. Among various oil palm biomass, i.e., empty fruit bunches (EFBs), mesocarp fibers (MFs), palm kernel shells (PKSs), oil

Abbreviations: AC, Ash content; AGF, 1,6-anhydro-β-D-glucofuranose; DGP, 1,4:3,6-dianhydro-β-D-glucopyranose; DTG, Derivative thermogravimetric analysis; EFB, Empty fruit bunch; FAME, Fatty acid methyl esters; FC, Fixed carbon; GC-MS, Gas chromatography–mass spectrometry; HHV, Higher heating value; LGA, Levoglucosan; LGO, Levoglucosenone; MC, Moisture content; MF, Mesocarp fiber; OPF, Oil palm frond; OPL, Oil palm leaf; OPT, Oil palm trunk; PKS, Palm kernel shell; PP, Polypropylene; TGA, Thermogravimetric analysis; VM, Volatile matter.

* Corresponding author.
E-mail addresses: jsunarso@swinburne.edu.my, jbarryjakasunarso@yahoo.com (J. Sunarso).

https://doi.org/10.1016/j.sajce.2022.12.001
Received 23 June 2022; Received in revised form 28 November 2022; Accepted 2 December 2022
Available online 5 December 2022
1026-9185/© 2022 The Author(s). Published by Elsevier B.V. on behalf of Institution of Chemical Engineers. This is an open access article under the CC BY license (http://creativecommons.org/licenses/by/4.0/).

Abbreviation

AGF	1,6-anhydro-β-D-glucofuranose
DGP	1,4:3,6-dianhydro-β-D-glucopyranose
EFB	Empty fruit bunch
HHV	Higher heating value
LGA	Levoglucosan
LGO	Levoglucosenone
MF	Mesocarp fiber
OPF	Oil palm frond
OPL	Oil palm leaf
OPT	Oil palm trunk
PKS	Palm kernel shell
PP	Polypropylene

palm trunks (OPTs), oil palm fronds (OPFs), and oil palm leaves (OPLs)) (Hamzah et al., 2019), OPTs have received less attention for research studies. OPTs are typically shredded and left in the plantations for natural decomposition following the replanting activities. The disposal of OPT can be costly given its bulky fibrous form (Khor et al., 2010). Thus, the push-felling and trunk-shredding followed by burning have been widely applied to the left-over OPTs during replanting activities, which resulted into undesirable greenhouse gas emissions (Abdullah and Sulaiman, 2013).

The utilization of OPT for pyrolysis oil production can reduce the negative impacts of these aforementioned practices. OPT-derived pyrolysis oil is carbon-neutral and more environmentally sustainable given its lower S and N content relative to fossil fuels (Palamanit et al., 2019). Nonetheless, high oxygen content of OPT generally translates to the formation of the oxygenated compounds (i.e., acids, ketones, and furans) and phenolic compounds in the resultant oil, which is undesirable since these compounds lower the energy content of the oil (Palamanit et al., 2019). To this end, OPT can be pyrolyzed together with other precursors such as plastics that contain large amount of carbon and hydrogen *via* co-pyrolysis to improve the formation of desired hydrocarbon and reduce the generation of oxygenated compounds (Rotliwal and Parikh, 2011). The wide use of plastics, especially for packaging, has created large amount of wastes and disposal issues. The resultant plastic wastes are mainly disposed of *via* landfill or domestic burning (Chen et al., 2021). Polypropylene (PP), which is rich in carbon and hydrogen content, in particular, is the second most abundant plastic used globally (Parku et al., 2020). During the co-pyrolysis, PP decomposition can provide hydrocarbon pools for the: (i) formation of hydrocarbons, (ii) reaction with the biomass-derived radicals to produce hydrocarbons, and (iii) reaction with the biomass-derived radicals to generate oxygenates such as alcohols and ketones (Al-Maari et al., 2021; Rotliwal and Parikh, 2011).

The existing studies on the OPT-derived pyrolysis oil have focused mainly on the effects of the operating conditions (i.e., feedstock types, temperature, and particle size) on the product yield (i.e., oil, char, and gas) and the characterization of pyrolysis oil (Abnisa et al., 2013; Chin et al., 2015; Mohammed et al., 2015; Sukiran et al., 2016). Although several studies reported the composition of the OPT-derived pyrolysis oil (Deris et al., 2006; Khor et al., 2010; Palamanit et al., 2019), none evaluated the reaction mechanism behind the formation of the main chemical compounds in the oil. The addition of PP into co-pyrolysis of biomass (i.e., EFB, OPF, waste wood chips, rice straw, and corn stover) or pure biomass chemical component (i.e., cellulose), on the other hand, has been covered in several studies (Al-Maari et al., 2021; Izzatie et al., 2016; Jeon et al., 2011; Ojha and Vinu, 2015; Wu et al., 2020). These studies highlighted the changes in the pyrolysis oil composition following PP addition and reported the increase of hydrocarbon constituents, the reduction of oxygenated components, and the formation of new chemical components such as ketones and alcohols (from the reaction between PP and biomass) in the products (Al-Maari et al., 2021; Ojha and Vinu, 2015). This work is the first study that combines OPT and PP as feedstocks of co-pyrolysis. Here, we evaluate the composition of oil produced from the pyrolysis of OPT (single feed) and co-pyrolysis of OPT and PP (binary feed). The changes in the composition of oil following the addition of PP are explained by discussing the reaction mechanism and interactions between the constituents of OPT and PP.

2. Materials and methods

2.1. Materials

OPT used in this work was collected from a local oil palm plantation in Saratok, Sarawak. After collection, OPT was pre-dried in the oven at 105 °C for 24 h and kept in sealed bags until further use. Before experiments, OPT was ground (Fritsch rotary mill, PULVERISETTE 14) and sieved (Fritsch sieve shaker, ANALYSETTE 3 PRO) to obtain samples with the particle size of 500 μm and below (Fig. 1(a)). The sieved OPT was then dried at 105 °C for 24 h and kept in the desiccators prior to the experiments. PP food containers were acquired locally and cut into smaller pieces and sieved by the sieve shaker (Fritsch, ANALYSETTE 3 PRO) to obtain samples with the particle size of 500 μm and below (Fig. 1(b)). The sieved PP was kept under ambient conditions prior to use.

2.2. Ultimate analysis

The ultimate analysis of OPT and PP was performed by using CHN analyzer (Leco, CHN 628). The carbon (C), hydrogen (H), and nitrogen (N) contents of the samples were obtained directly from the analyzer while the ash content (AC) was obtained from the proximate analysis. The oxygen content (O) was obtained *via* the difference in weight percentage as follows:

$$O(wt.\%) = 100(wt.\%) - C(wt.\%) - H(wt.\%) - N(wt.\%) - AC(wt.\%) \quad (1)$$

2.3. Proximate analysis

Proximate analysis was performed using the simultaneous thermal analyzer (Perkin Elmer, STA 8000) to determine the moisture content (MC), volatile matter (VM), fixed carbon (FC), and ash content (AC) of OPT and PP. The procedure was adapted from ASTM D7582–12 (ASTM International, 2012), whereby approximately 10 mg of sample was weighed in the sample pan of the thermal analyzer. The analysis was programmed as follows:

(i) Sample was held at 30 °C for 4 min.
(ii) Sample was heated from 30 to 107 °C with a heating rate of 10 °C min^{-1} and a dwelling time of 9 min at 107 °C.
(iii) Sample was heated from 107 to 950 °C with a heating rate of 28 °C min^{-1} and held for 7 min at 950 °C.
(iv) Temperature was then reduced to 600 °C.

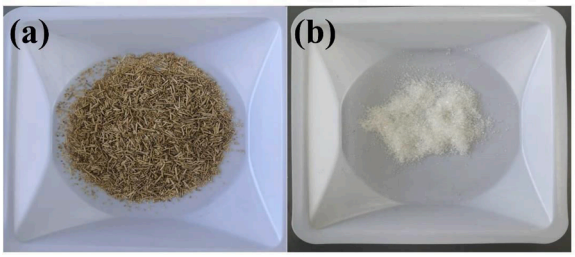

Fig. 1. (a) The sieved oil palm trunk (OPT) and (b) polypropylene (PP) for experimental runs.

(v) The purging gas was switched from nitrogen to oxygen at 600 °C.
(vi) Sample was then heated from 600 to 750 °C at 2.5 °C min^{-1} and held for 18 min at 750 °C in oxygen atmosphere.

Step (i)-(ii), (iii), and (iv-vi) were for the determination of MC, VM, and AC, respectively. The FC was calculated *via* the difference in weight percentage as follows:

$$FC(wt.\%) = 100(wt.\%) - MC(wt.\%) - VM(wt.\%) - AC(wt.\%) \quad (2)$$

The flow rates of nitrogen and oxygen were 20 mL min^{-1} throughout the analysis.

2.4. Lignocellulosic content analysis

The extractives of OPT was determined through Soxhlet extraction method with the ethanol used as the solvent (Sluiter et al., 2005). Approximately 2–10 g of raw OPT sample was added into the cellulose thimble while 190 mL of ethanol was added into the round-bottom flask. Then, the Soxhlet apparatus was assembled. The Soxhlet extraction was conducted by achieving a minimum of 6–10 siphon cycles per hour with the reflux period of 16–24 h. Once the reflux was completed, the Soxhlet apparatus was left for cooling down to room temperature. The cellulose thimble containing OPT sample was then taken out from the Soxhlet apparatus and washed with distilled water. After this, it was dried at 105 °C for 24 h. The extractive of OPT was determined *via* the difference in weight percentage between raw OPT and extractive-free OPT after drying.

$$Extractives\ (wt.\%) = \frac{\text{Initial mass of OPT sample (g)} - \text{Mass of OPT sample after drying (g)}}{\text{Initial mass of OPT sample (g)}} \times 100\% \quad (3)$$

The procedure of hemicellulose extraction was adapted from Yang et al. (2006). Approximately 1 g of extractive-free OPT sample was added into the round-bottom flask and followed by 150 mL of sodium hydroxide solution with the concentration of 0.5 mol L^{-1}. The sample was heated at 80 °C for 3.5 h using reflux apparatus. After the sample was cooled down to room temperature, it was washed with distilled water until the pH of distillate reached 7. The washed sample was then dried at 105 °C for 24 h. The hemicellulose content was obtained *via* the difference between the initial mass and mass of extractive-free OPT after drying.

$$Hemicellulose(wt.\%) = \frac{\text{Initial mass of extractive} - \text{free OPT (g)} - \text{Mass of extractive} - \text{free OPT after drying (g)}}{\text{Initial mass of extrative} - \text{free OPT (g)}} \times 100\% \quad (4)$$

The lignin content was determined based on the standard procedure from NREL (Sluiter et al., 2012) and TAPPI T222 om-02 (TAPPI, 2006). Approximately 0.2 g of extractive-free OPT sample was added in a 100 mL beaker. 3 mL of cold 72% sulfuric acid (10–15 °C) was added gradually and the sample was stirred and macerated with a glass rod simultaneously. Then, the beaker was covered with a petri dish and placed in a bath of 2 °C during the dispersion of the sample for 2 h. After that, 112 mL of distilled water was added to dilute the sulfuric acid containing sample to 3% concentration with the total volume of 115 mL for the solution. Next, the solution was boiled for 4 h and its constant volume (115 mL) was maintained during boiling by the addition of hot water frequently. After 4 h of boiling, the insoluble material (insoluble lignin) in the solution was allowed to settle. Then, the supernatant solution was collected carefully using micropipette without stirring up the precipitate (insoluble lignin). The collected supernatant solution was then used to determine the content of acid soluble lignin of OPT *via* UV–Visible spectrophotometer (Perkin Elmer, Lambda 35) at 205 nm. (Refer to **Supplementary Information** for calculation). The remaining solution with insoluble lignin was filtered and washed using hot water to remove sulfuric acid. The washed sample was then dried at 105 °C for 24 h. The difference between initial and mass after the drying was obtained to determine the insoluble lignin content of extractive-free OPT.

$$Total\ lignin\ (wt.\%) = Acid\ soluble\ lignin\ (wt.\%) + Acid\ insoluble\ lignin\ (wt.\%) \quad (5)$$

The cellulose content of extractive-free OPT was then determined as follows:

$$Cellulose(wt.\%) = 100(wt.\%) - hemicellulose(wt.\%) - total\ lignin(wt.\%) \quad (6)$$

2.5. Thermal analysis

The thermal behaviors of OPT and PP were analyzed *via* thermogravimetric method using simultaneous thermal analyzer (Perkin Elmer, STA 8000). The samples were weighed in the sample pan of the analyzer and then heated from 50 to 900 °C at a heating rate of 10 °C min^{-1}. Nitrogen gas flow rate was maintained at 20 mL min^{-1} during the analysis.

2.6. Higher heating value (HHV) analysis

The higher heating values (HHVs) of OPT and PP were measured using a bomb calorimeter (IKA, C200). The sample was weighed and put into the combustion crucible. A cotton thread was tied on the ignition wire of the decomposition vessel and put into the vessel together with the crucible. The vessel was filled with oxygen through the oxygen filling station until the pressure in the vessel reached 30 bar. Then, the vessel was placed in the main machine, and the information was input into the software before the analysis was started. Once it was completed, the HHV value of the sample was obtained from the software and recorded.

2.7. Pyrolysis experiments

Pyrolysis experiments were performed in a horizontal tube furnace

(MTI, GSL-1100X). Nitrogen was used as the carrier gas at a flow rate of 400 mL min^{-1} to create an inert condition during the experiments. 3 g of OPT sample was loaded into the reactor and purged with nitrogen for 5 min. Then, the purged reactor tube was heated to the target temperature (i.e., 500, 600, and 700 °C) at a heating rate of 10 °C min^{-1}. The sample was held at the target temperature for 40 min. Following the hold duration, the reactor was cooled down to 200 °C with continuous nitrogen flow. A cold trap submerged in an ice bath that was installed at the outlet of the tube reactor served as the condenser for collecting pyrolysis oil. Liquid fractions generated during the reaction were collected and stored at 2–7 °C until further analysis. The non-condensable gasses were vented into the atmosphere. During the co-pyrolysis experiments, 3 g of OPT and PP mixture sample (weight ratio of OPT:PP of 1:1) was used. Then, the same operating procedure (i.e., heating rate, the flow rate of nitrogen gas, temperature, and hold time) was applied in the co-pyrolysis experiments. The product yield obtained from the experiments was calculated using Eqs. (7)-(9).

$$Pyrolysis\ oil\ yield(wt.\%) = \frac{\text{Mass of pyrolysis oil obtained (g)}}{\text{Total mass of sample (g)}} \times 100\% \quad (7)$$

$$Char\ yield(wt.\%) = \frac{\text{Mass of char obtained (g)}}{\text{Total mass of sample (g)}} \times 100\% \quad (8)$$

$$Gas\ yield(wt.\%) = 100(wt.\%) - pyrolysis\ oil\ yield(wt.\%) - char\ yield(wt.\%) \quad (9)$$

2.8. Gas chromatography-mass spectrometry (GC-MS) analysis

The pyrolysis oil composition was analyzed using gas chromatography-mass spectrometer (GC–MS) analysis (Agilent, 6890 N) with HP-5MS column (Agilent, 30 m length × 0.25 mm inner diameter × 0.25 μm film thickness). Helium gas at a 1 mL min^{-1} flow rate and a pressure of 7.04 psi were applied to the equipment. A split ratio of 50:1 was adopted for the analysis. The oven was programmed to be heated to 40 °C firstly and held at 40 °C for 3 min. Next, it was ramped from 40 to 200 °C at 8 °C min^{-1} and held at 200 °C for 10 min. Then, another ramping from 200 to 220 °C at 10 °C min^{-1} was performed. The temperature was kept at 220 °C during analysis. Prior to analysis, 0.2 g of pyrolysis oil was diluted in 10 mL of acetone. The diluted sample was filtered by a syringe filter, transferred into the GC sample vial, and injected into the equipment through auto-injection mode for the analysis. Chemical compounds in pyrolysis oil were identified by comparison with entries in the NIST08 mass spectral data library. Phenol was used as the chemical standard for the calibration. The phenol was prepared in three different concentrations (i.e., 0.426, 0.644, and 0.98 mg mL^{-1}) to construct the calibration curve.

Table 1
OPT and PP analyses results.

Properties		OPT	PP
Ultimate analysis (wt.%)[a]	**Carbon content**	43.20	85.03
	Hydrogen content	6.42	13.99
	Nitrogen content	0.52	0.09
	Oxygen content	43.37	0.00
Proximate analysis (wt.%)	**Moisture content**	0.98	0.00
	Volatile matter	89.02	96.48
	Fixed carbon	3.51	2.63
	Ash content	6.49	0.89
Lignocellulosic content analysis (wt.%)	**Hemicellulose**	41.66	–
	Cellulose	26.83	–
	Lignin	12.94	–
	Extractives	18.57	–
HHV analysis (MJ kg^{-1})		17.68	46.79

[a] Sulfur-free basis.

3. Results and discussion

3.1. Materials characterization

Table 1 presented the results of ultimate, proximate, lignocellulosic content, and HHV analyses of OPT and PP. The CHNO content of OPT obtained from the ultimate analysis was consistent with the literatures in particular for its high oxygen content (Khor et al., 2010; Palamanit et al., 2019). High oxygen content of OPT likely led to the production of pyrolysis oil with high amount of oxygenated compounds (i.e., acids, ketones, and furans) and phenolic compounds. Conversely, PP had lower oxygen content and higher carbon and hydrogen contents than OPT. This allowed PP to be used as a co-feeding material for co-pyrolysis with OPT since it could supply carbon and hydrogen needed to form the desired hydrocarbons in the pyrolysis oil (Al-Maari et al., 2021; Ojha and Vinu, 2015).

The moisture contents of OPT and PP were 0.98 and 0 wt.%, respectively, which lied within the suggested moisture content range in the feedstock selection for high pyrolysis oil production (i.e., 10 wt.% and below) (Abnisa and Wan Daud, 2014). Moreover, the volatile matters of OPT (89.02 wt.%) and PP (96.48 wt.%) were anticipated to contribute to the pyrolysis oil production during co-pyrolysis. The ash content of both feedstocks was considered low, which was favorable to get high yield of pyrolysis oil (Fukuda, 2015). PP had a 2.6-fold higher HHV value than OPT, which reflected its higher carbon and hydrogen content and lower ash content (Devasahayam et al., 2019). For the lignocellulosic content of OPT, its hemicellulose, cellulose, and lignin obtained was 41.66, 26.83, and 12.94 wt.%, respectively, of which their depolymerization during pyrolysis contributed to the formation of different chemical compounds in the oil. Hemicellulose and cellulose mainly contributed to the ketones and furans formation while lignin contributed to the production of phenol and its derivatives (Jiang et al., 2010; Zhao et al., 2017).

3.2. Thermal analysis

Fig. 2 and Fig. 3 showed the respective weight loss profile (TGA) and derivative weight loss profile (DTG) of OPT, PP, and the mixture of OPT and PP obtained from thermogravimetric analyses in nitrogen (inert) atmosphere. The peaks detected below 150 °C in DTG profiles could be attributed to the moisture removal from the feedstocks (Fig. 3) (Soh et al., 2020).

For OPT, three peaks were observed between 187–235, 235–387, and 800–900 °C, respectively (Fig. 3). Hemicellulose had the lowest thermal stability among the three main biopolymers of lignocellulosic

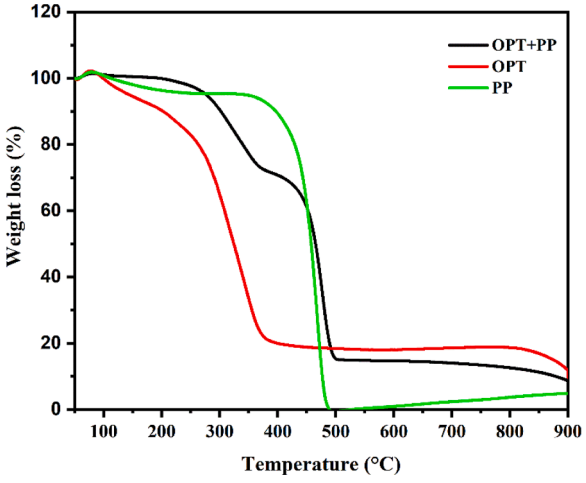

Fig. 2. TGA profiles of OPT, PP, and the mixture of OPT and PP in nitrogen atmosphere.

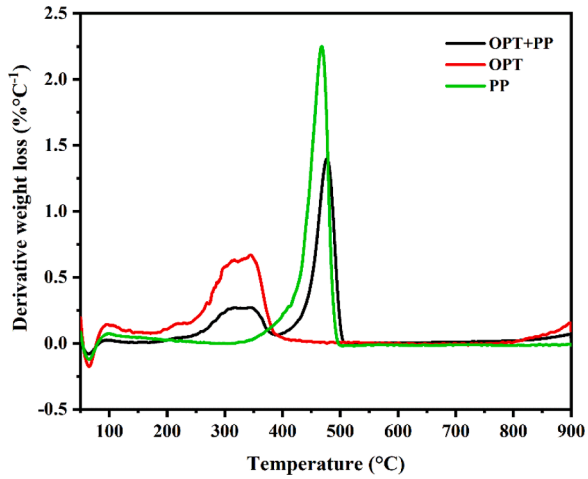

Fig. 3. DTG profiles of OPT, PP, and the mixture of OPT and PP in nitrogen atmosphere.

biomass (i.e., cellulose, hemicellulose, and lignin), its decomposition of which corresponded to the first peak that appeared between 187 and 235 °C (Fig. 3) (Yang et al., 2006). Lignin decomposition started at 180 °C, thus minor lignin decomposition may also occur in this temperature range (Yang et al., 2006). The maximum weight loss of up to 64.8% that occurred between 235–387 °C was due to the overlapping of hemicellulose, cellulose, and lignin decomposition (Fig. 2) (Zhao et al., 2017). Above 400 °C, the weight loss of OPT was mainly due to the decomposition of lignin, which has the highest thermal stability with a broad decomposition temperature range from 180 to 900 °C (Fig. 2) (Gašparovič et al., 2010).

In PP case, only one sharp peak was observed in the temperature range of 340 to 500 °C (Fig. 3) that was associated to a weight loss of up to 95% (Fig. 2). Similar observation of single peak in DTG curve of PP was also reported in the literature (Singh et al., 2019). Within the temperature range of 340 to 500 °C, the thermal breakage of the carbon-carbon bonds between the monomers of PP was enhanced as temperature rose. The increase of temperature promoted the formation of gaseous products and reduced the solids' yield (H.-S. Kim et al., 2006). However, beyond 500 °C, an unexpected weight gain appeared, which was most likely caused by the reaction between the additives' residues in PP sample during TGA analysis (Fig. 2). Nonetheless, further studies were required to better understand the commercial PP composition since the types of additives used may vary depending on the manufacturing process.

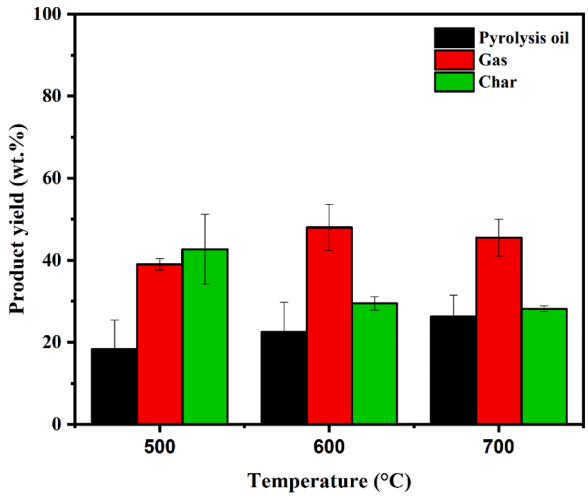

Fig. 4. Product yield from the pyrolysis of OPT.

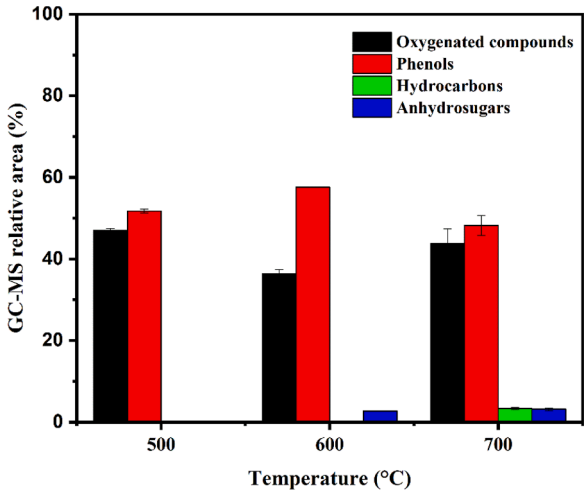

Fig. 5. Oil composition from pyrolysis of OPT at 500, 600, and 700 °C.

For the OPT and PP mixture, multiple peaks were observed from the DTG profiles in the temperature range of 187 to 507 °C (Fig. 3) that correlated with the weight loss of 85% from its initial weight (Fig. 2). The peaks that appeared between 187 and 387 °C came from the decomposition of hemicellulose, cellulose, and lignin while the sharp peak that was present between 387 and 507 °C corresponded to the PP decomposition (Fig. 3). A minor peak was also observed from DTG curve of the mixture in between 800 and 900 °C (Fig. 3), attributable to the lignin decomposition from OPT. The residues that remained upon heating beyond 387 and 507 °C for OPT and the mixture of OPT and PP, respectively, correlated well with the fixed carbon and ash contents in OPT that were thermally stable up to 900 °C (Brebu et al., 2010).

3.3. Pyrolysis of OPT

This section mainly discussed the product yield and oil composition obtained from the pyrolysis of OPT between 500 and 700 °C. The formation mechanisms of the main oil composition detected from the OPT-derived oil were also evaluated in this section.

3.3.1. Product yield

Fig. 4 showed the product yield (i.e., oil, gas, and char) obtained from the pyrolysis of OPT in the temperature range of 500–700 °C. Pyrolysis oil yield increased from 18.33 to 26.33 wt.% as the temperature increased from 500 to 700 °C, implying that lignin decomposition was the main contributor within this temperature range as supported by the GC–MS results (Fig. 5). The highest pyrolysis oil yield of 26.33 wt.% was obtained at 700 °C with a solid char yield of 28.17 wt.%. At 700 °C, the highest pyrolysis oil yield was contributed by the phenolic and oxygenated compounds as the major composition in the oil (Fig. 5). An increase in the amount of oxygenated compounds by 8% was observed when temperature was increased from 600 to 700 °C. A reduction in the amount of phenolic compounds by 9% due to their conversion into the hydrocarbons (3.33%) was also shown from 600 to 700 °C, contributing to the highest oil yield at 700 °C. The decrease of solid char yield from 42.67 to 28.17 wt.% with the increase of temperature from 500 to 700 °C was due to the enhanced secondary decomposition of char at higher temperature (Khor et al., 2010). Gas yield, on the other hand, exhibited a maximum trend with the highest yield of 48 wt.% recorded at 600 °C.

3.3.2. Pyrolysis oil composition

The constituents of pyrolysis oil from OPT were analyzed using GC–MS, and their relative amounts were presented in terms of GC–MS

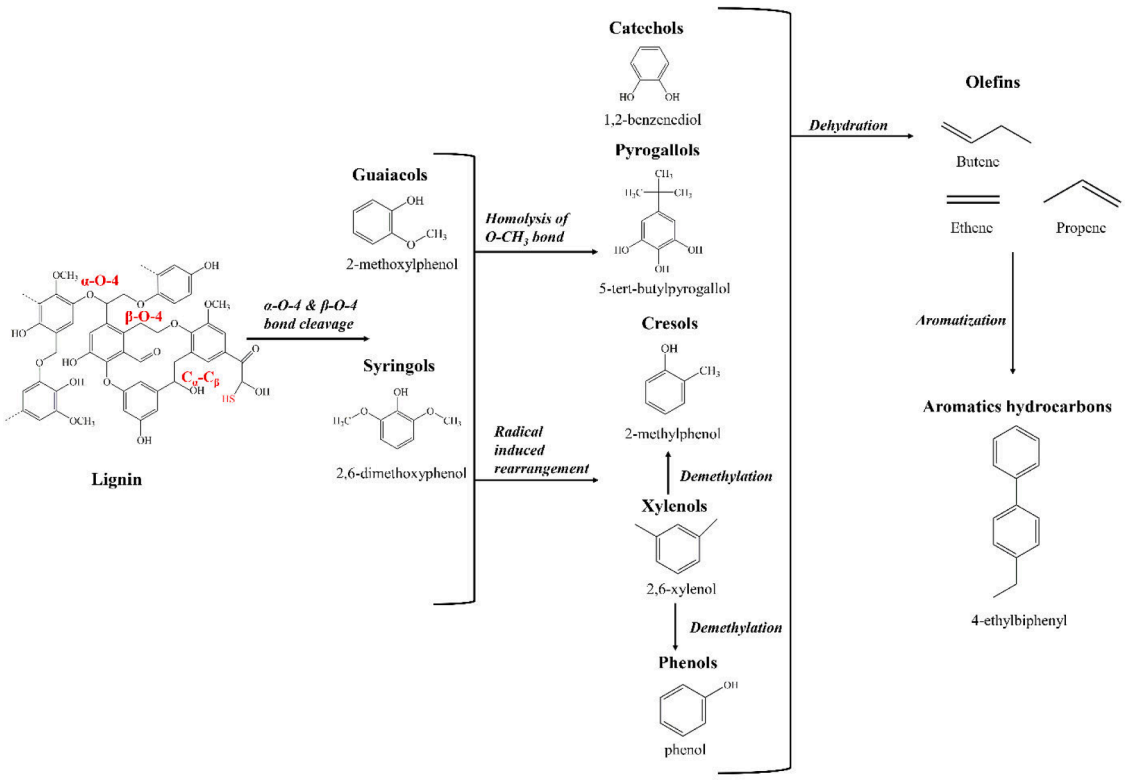

Fig. 6. Proposed reaction mechanism of phenolic compounds and hydrocarbons formation via lignin decomposition. Modified with permission from Jiang et al. (2010) and J.-Y. Kim et al. (2020).

relative area (Fig. 5). Between 500 and 700 °C, the OPT-derived pyrolysis oil mainly consisted of phenolic compounds (51.77–57.78%) and oxygenated compounds (36.31–46.99%) with smaller portion of sugars (2.7–3.15%) and hydrocarbons (3.33%). High content of oxygenated and phenolic compounds in OPT-derived pyrolysis oil was anticipated given the high oxygen content of 49.86 wt.% in OPT as revealed by the above ultimate analysis result in Table 1.

A maximum GC–MS relative area of phenolic compounds of 57.58% was obtained at 600 °C, which was reduced to 48.21% upon heating to 700 °C. The production of phenolic compounds was mainly from the lignin decomposition, which began *via* the cleavage of ether bonds (i.e., β-O-4 and α-O-4 bonds) to form the lignin monomers (i.e., guaiacols and syringols) (Jiang et al., 2010). The conversion of the lignin monomers into the phenolic compounds was through the homolysis of O—CH_3 bonds, radical-induced rearrangement, and demethylation, as illustrated in Fig. 6. The detected phenolic compounds from the pyrolysis oil include phenol, 2-methyl-phenol, 2,6-dimethoxy-phenol, 2,6-dimethoxy-4-(2-propenyl)-phenol, 2-methoxy-4-vinyl-phenol, 5-tert-butylpyrogallol, 1,2-benzenediol, and 3-methoxy-1,2-benzenediol, which were consistent with the findings of the other studies on the pyrolysis of OPT (Deris et al., 2006; Palamanit et al., 2019). Above 600 °C, the reduction in the content of phenolic compounds reflected their conversion into hydrocarbons such as aromatic hydrocarbons. At higher temperatures, the cracking, dehydration, and decarbonylation of the phenolic compounds occurred to generate small olefins. After that, these small olefins further underwent aromatization to form aromatic hydrocarbons such as 4-ethylbiphenyl as detected in the pyrolysis oil (Charisteidis et al., 2019; J.-Y. Kim et al., 2020).

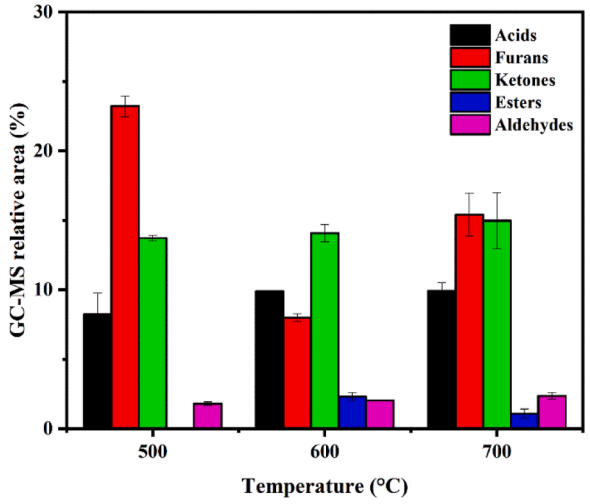

Fig. 7. Oxygenated compounds detected in OPT-derived pyrolysis oil from 500 to 700 °C.

These phenolic compounds generally can be used as the primary precursors in the manufacturing of resins (e.g., phenol-formaldehyde resins), adhesives, nylon, and synthetic fibers (Machado et al., 2022). They also can be converted into valuable aromatic hydrocarbons, such as benzene, toluene, and xylene that are important in petrochemical industry (Suriapparao et al., 2020). Benzene can be applied as the precursors in the styrene production for making latex, synthetic rubber, and polystyrene resins (Niziolek et al., 2016).

Ketones (13.73–14.98%) and furans (8–23.23%) were the major oxygenated compounds detected in the OPT-derived pyrolysis oil (Fig. 7). During hemicellulose decomposition, the cyclic ketones were produced through the cyclization of the linear carbon chains (i.e., the reaction of intermediates with the hexatomic rings). On the other hand, linear ketones formation took place *via* the breakage of linear carbon chains (Fig. 8) (Wang et al., 2013). The formation of furans was mainly associated with the formation of anhydrosugars intermediates (i.e., levoglucosan (LGA) and 1,4:3,6-dianhydro-β-D-glucopyranose (DGP)) during the depolymerization of cellulose (Fig. 9). The dehydration,

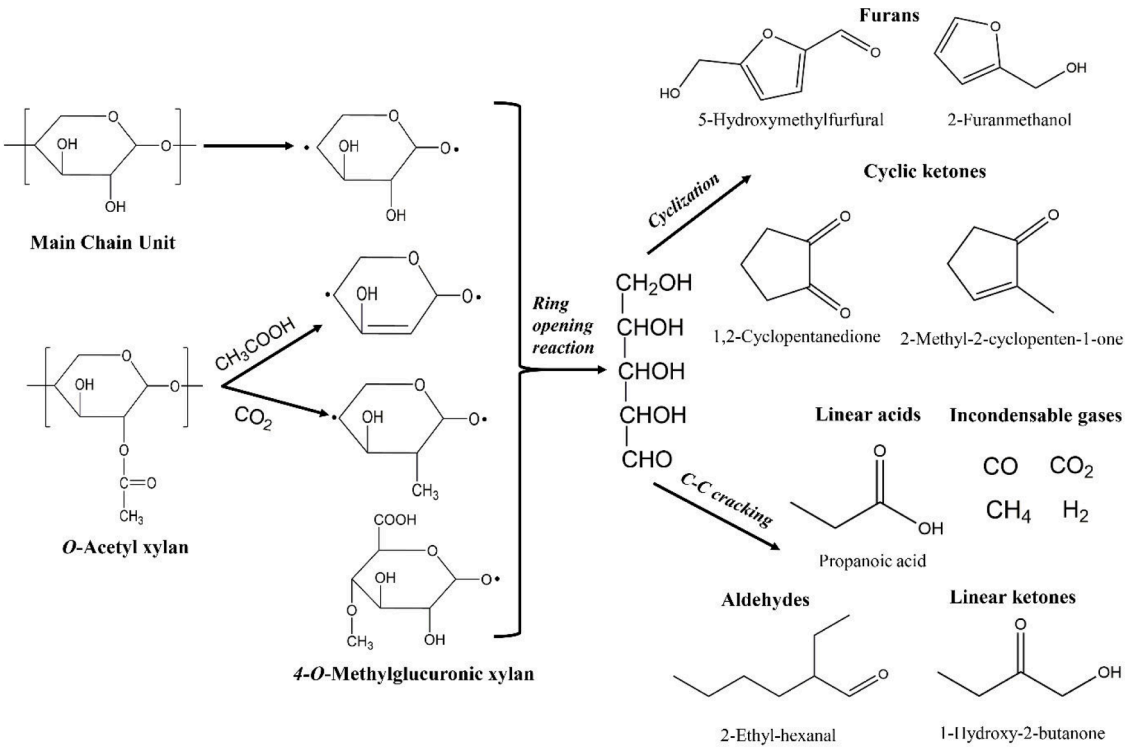

Fig. 8. Proposed reaction mechanism of hemicellulose decomposition for the formation of ketones and furans. Adapted from Wang et al. (2013).

decarboxylation, and decarbonylation of the anhydrosugars resulted in the formation of furans such as furfural, 2-furanmethanol, and 5-hydroxymethylfurfural (Lin et al., 2009; Zhao et al., 2017). Besides that, the formation of furans was also contributed by the cyclization of the linear chains (i.e., intermediates from the depolymerization of hemicellulose) (Fig. 8) (Wang et al., 2013). The conversion of the anhydrosugars into furans was the highest at 500 °C as the maximum GC–MS relative area of furans (23.23%) was recorded (Fig. 7), with no anhydrosugars detected in the OPT-derived pyrolysis oil (Fig. 5). The increase of temperature led to the reduction in the content of furans due to the lower conversion from anhydrosugars into the furans. This was consistent with the presence of anhydrosugars in the pyrolysis oil at 600 and 700 °C (Fig. 5).

Both ketones and furan compounds are considered as the valuable platform chemicals in many industries. Jaya et al. (2022) reported the application of cyclic ketones (i.e., cyclopentanone and its derivatives) in the synthesis of pesticides, fungicides, and pharmaceuticals. Besides, Li et al. (2021) also reported the potential routes in the production of aviation fuel through the aldol condensation and hydrogenation of biomass-derived ketones. For furan compounds such as furfural, about 62% are converted into the furfuryl alcohol and its derivatives annually for the production of foundry resins, furan fiber-reinforced plastics (for piping) in global market (Mandalika et al., 2014). The by-product, furoic acid produced during this conversion process also can be used in the pharmaceutical, fragrance, flavor, and agrochemical industries (Kohli et al., 2019).

The presence of acids (i.e., linear short-chain acids, long-chain acids, and aromatic acids) were mainly attributed to the decomposition of hemicellulose and lignin. The increase in the overall acidic components from 500 to 700 °C (Fig. 7) was contributed by long chain and aromatic acids in the pyrolysis oil. Short-chain linear acids such as propanoic acid formed from the carboxylation group's cleavage from the *O*-acetyl xylan units, which also resulted in the release of carbon dioxide gas during the thermal degradation stage of hemicellulose (Fig. 8) (Stefanidis et al., 2014; Wang et al., 2013). The long-chain acids (i.e., palmitic acid) and aromatic acids (i.e., benzoic acid, 4-hydroxy-3-methoxy-benzoic acid, and 3-(4-hydroxy-3-methoxyphenyl)-2-propenoic acid) were obtained from the breakage of ether bonds and the side chain of the lignin (Zhao et al., 2017) (Fig. 10).

These biomass-derived acids are common and important chemicals for variety of applications in many industries. Gonzalez-Garcia et al. (2017) reported the commercial application of propanoic acid in the production of propionate for the uses in food preservative and cleaning products. Mank and Polonska (2016) mentioned the application of palmitic acid as the bioactive ingredient in the cosmetics products. Prinsen et al. (2018) reported that the production of renewable biodiesel, which is also called as fatty acid methyl ester (FAME) *via* the esterification of palmitic acid (methyl palmitate is the FAME produced from this process). Another work by Duongbia et al. (2022) also reported the potential of the catalytic hydrotreating of palmitic acid with the selected catalysts for the production of oleochemicals (i.e., fatty acid ester and fatty alcohol). Both fatty acid ester and fatty alcohol can be further processed for the manufacturing of detergent, lubrication, solvent, and surfactant. Nevertheless, benzoic acid and its derivatives are mostly used in food preservatives, plasticizers, dyes, and medicines (Xin Zhang et al., 2013).

Light oxygenates such as aldehydes (1.8–2.36%) were also detected from the OPT-derived pyrolysis oil at between 500 to 700 °C (Fig. 7), which were produced *via* the fragmentation of anhydrosugars (from cellulose) and linear carbon chains (intermediates of hemicellulose), as illustrated in Fig. 8 and Fig. 9 (Lin et al., 2009; Usino et al., 2020; Wang et al., 2013). In addition, a low portion of esters (1.1–2.3%) such as 4-methoxy-benzoic acid methyl ester was detected in pyrolysis oil, which was originated from the esterification of aromatic acids and alcohols during the process.

3.4. Co-pyrolysis of OPT

This section presented the findings on the product yield and oil composition after the addition of PP into co-pyrolysis of OPT between 500 and 700 °C. The changes in oil composition following the addition of PP were explained by discussing the reaction mechanism and interactions between the constituents of OPT and PP.

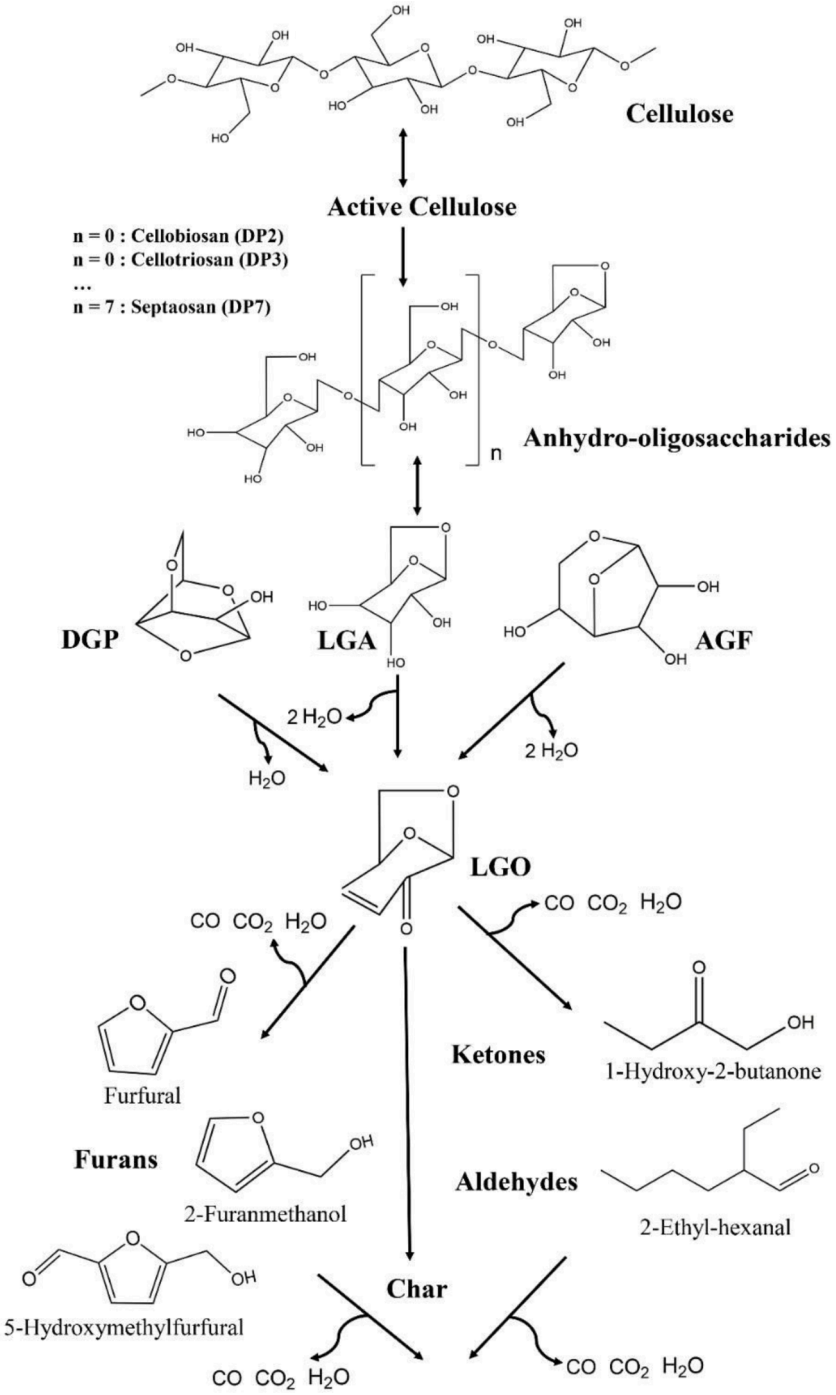

Fig. 9. Proposed reaction mechanism for cellulose decomposition. Modified with permission from Lin et al. (2009).

3.4.1. Product yield

Fig. 11 depicted the effect of temperature on the product yield of the co-pyrolysis of OPT and PP between 500 and 700 °C. The increase in the yield of pyrolysis oil was observed with temperature rise from 500 to 600 °C with a maximum oil yield of 16.17 wt.% obtained at 600 °C. This was then followed by a reduction in oil yield to 11.50 wt.% at 700 °C. The decrease of char yield from 33.50 to 19.33 wt.% occurred with an increase in the temperature from 500 to 700 °C. On the other hand, gas yield of 50.42–69.17 wt.% was obtained between 500 and 700 °C. Below 700 °C, high thermal decomposition of the OPT and PP was responsible for the production of volatiles that maximized the pyrolysis oil yield. At 600 °C, the highest oil yield was mainly contributed by the formation of the phenolic compounds (45.16%) and hydrocarbons (10.2%) (Fig. 12). On the other hand, although a major reduction in the amount of oxygenated compounds of 17% was observed as the temperature was increased from 500 to 600 °C (Fig. 12), the oxygenated compounds were still present as the major component (34.9%) in the oil. Above 700 °C, the secondary decomposition of volatiles and char into lighter components occurred that generated more gaseous products (Wu et al., 2020).

3.4.2. Pyrolysis oil composition

Fig. 12 presented the pyrolysis oil composition from the co-pyrolysis of OPT and PP between 500 and 700 °C. During the co-pyrolysis, the chemical compounds in the pyrolysis oil were formed *via* a series of reactions, which included (i) OPT decomposition (hemicellulose, cellulose, and lignin), (ii) PP decomposition, and (iii) intermolecular

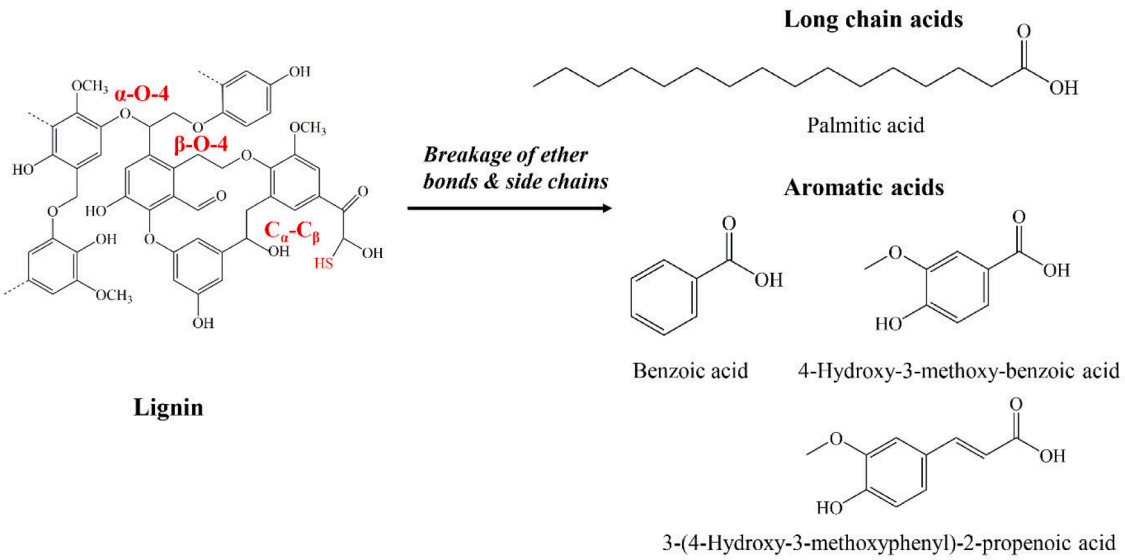

Fig. 10. Acids formation from lignin depolymerization (Zhao et al., 2017).

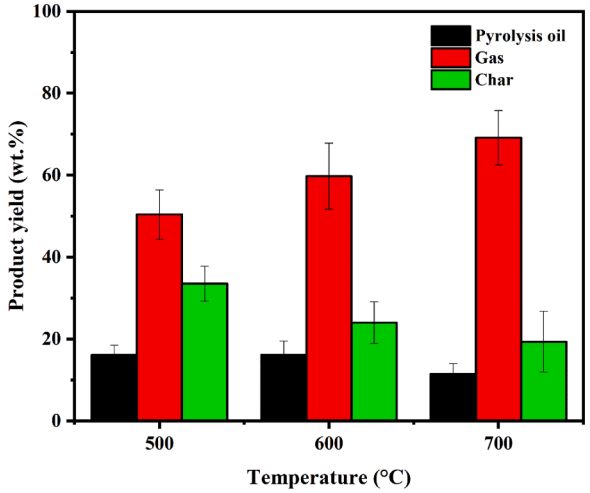

Fig. 11. Product yield from co-pyrolysis of OPT and PP.

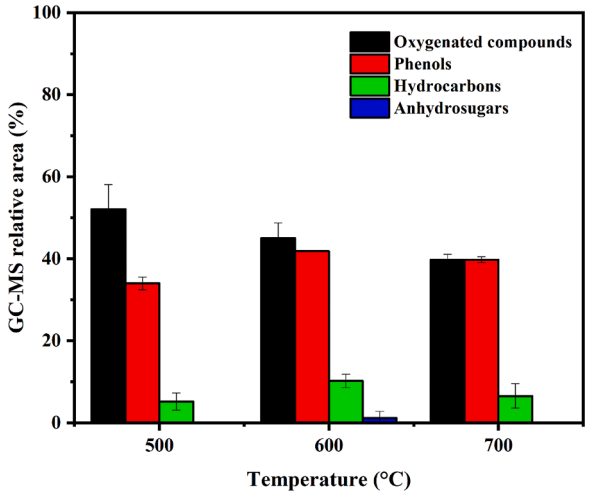

Fig. 12. Pyrolysis oil composition from co-pyrolysis of OPT and PP from 500 to 700 °C.

reactions between OPT, PP, and their intermediate products, as suggested by Xue et al. (2017). Phenolic (34.01–41.85%) and oxygenated compounds (39.74–52.10%) remained as the dominant pyrolysis oil components in the co-pyrolysis of OPT and PP as depicted by the GC–MS results in Fig. 12. Besides that, hydrocarbons (5.19–10.22%) and anhydrosugars (1.18%) were also detected in the pyrolysis oil.

The formation of phenolic compounds was contributed by the lignin depolymerization *via* similar reaction mechanism as shown in Fig. 6. Hydrocarbons (i.e., olefins and aliphatic hydrocarbons) detected in pyrolysis oil were mainly from the decomposition of PP *via* the reaction mechanism illustrated in Fig. 13. The mechanism involved a series of reactions, which included random chain scission, β-scission (i.e., mid-chain and end chain β-scission), radical recombination, and hydrogen transfer reactions (Kruse et al., 2003; Singh et al., 2019; Xue et al., 2017). The decrease of hydrocarbons content with temperature rise to 700 °C (Fig. 12) was most likely caused by the higher conversion of hydrocarbons into gaseous hydrocarbons *via* β-scission and hydrogen chain transfer reactions at higher temperature (Wu et al., 2020). Hydrocarbons are important precursors in petrochemical industry for variety of usage. Generally, hydrocarbons can be used as solvents in household cosmetics, chemicals, and pesticides, the manufacturing of plastics, rubber, fertilizers, detergents, fiber raw materials and so on (Park et al., 2019).

In oxygenated compounds case, GC–MS results indicated an increase in content from 500 to 600 °C with the highest GC–MS relative area of 52.10% attained at 500 °C (Fig. 12). This was followed by the reduction in GC–MS relative area to 39.74% at 700 °C. The increase in the content of long-chain acids (i.e., palmitic acid and tetradecanoic acid) in the pyrolysis oil with temperature rise indicated the enhancement on the breakage of ether bonds and side chain of the lignin at higher temperature (Fig. 10) (Zhao et al., 2017). The highest GC–MS relative area of furans (20.39%) was obtained at 500 °C (Fig. 14). This correlated with enhanced deoxygenation of anhydrosugars into furans in the presence of PP-derived radicals (Lin et al., 2020). In the presence of PP-derived radicals during co-pyrolysis, the formation of ketones occurred through two main routes, which were (i) the enhancement of hemicellulose and cellulose depolymerization by the PP-derived radicals (Lin et al., 2020) and (ii) the interactions between carbonyl radicals from hemicellulose and cellulose and PP-derived radicals for the formation of new ketones such as 4-isopropyl-1,3-cyclohexanedione, and 2-acetylcyclopentanone (Fig. 13) (Ojha and Vinu, 2015). In addition, new oxygenated compounds were detected that were absent in pyrolysis of OPT, i.e., alcohols such as 1-heptacosanol and 2-hexyl-1-decanol

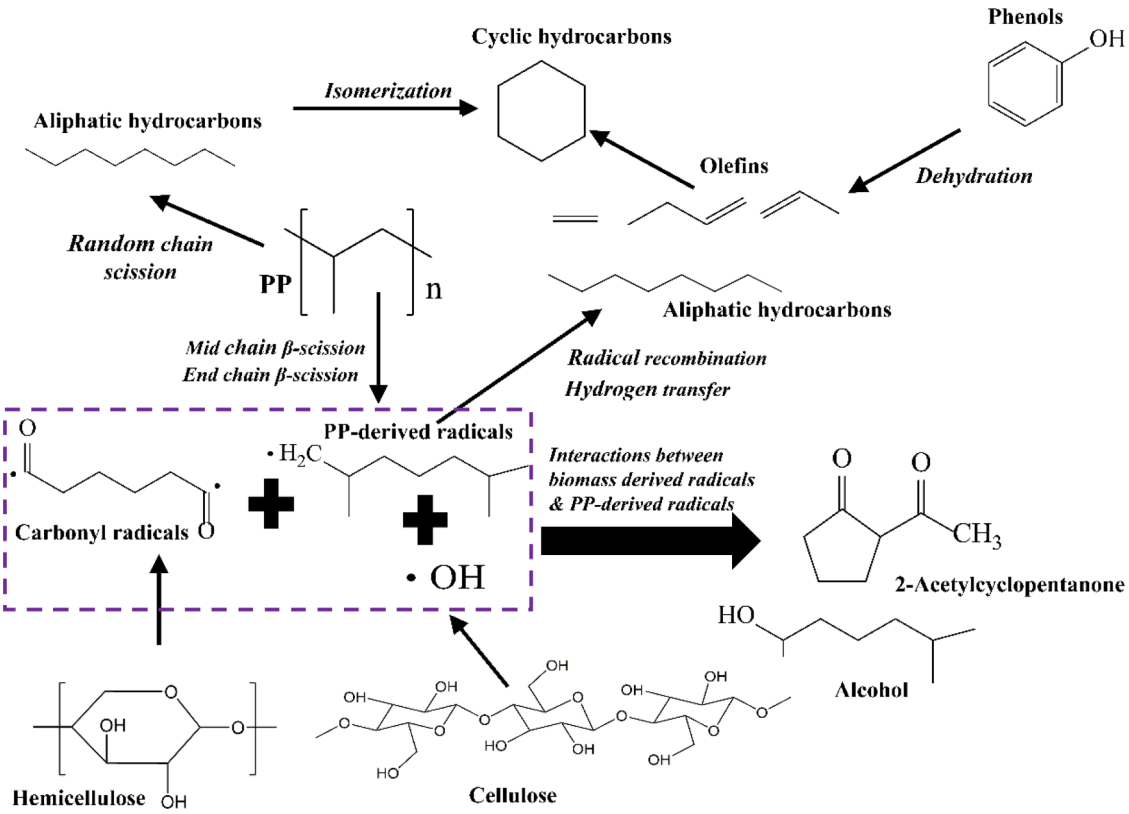

Fig. 13. Proposed mechanism of PP decomposition and interactions with OPT. Modified with permission from Al-Maari et al., (2021); Ojha and Vinu (2015), and Xue et al., (2017).

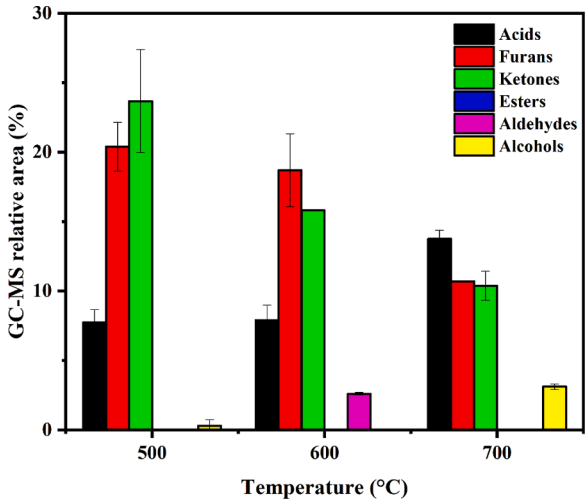

Fig. 14. Oxygenated compounds from oil during co-pyrolysis of OPT and PP.

(compare Fig. 14 to Fig. 7). They were generated from the intermolecular reactions between hydroxyl radicals from cellulose and PP-derived radicals (Fig. 13), which was consistent with the findings from the literatures (Al-Maari et al., 2021; Ojha and Vinu, 2015; Xue et al., 2017).

4. Conclusion

The pyrolysis of OPT (single feed) and co-pyrolysis of OPT with PP (binary feed) were successfully carried out between 500 and 700 °C. Several characterization tests, i.e., ultimate, proximate, lignocellulosic content, HHV, product yield, and GC–MS analyses were performed on the feed materials and products. PP had higher carbon, hydrogen, and volatile contents relative to OPT, thus allowing PP to become the hydrocarbon source in co-pyrolysis to improve the hydrocarbon content in the resultant pyrolysis oil. The highest pyrolysis oil yields of 26.33 wt.% and 16.17 wt.% from pyrolysis of OPT at 700 °C and co-pyrolysis of OPT at 600 °C with PP, respectively, were obtained. The main chemical constituents in the OPT-derived pyrolysis oil were phenolic and oxygenated compounds formed *via* the depolymerization of hemicellulose, cellulose, and lignin in OPT. For co-pyrolysis, the phenolic and oxygenated compounds were still the dominant constituents in oil, but their slight decrease in amount was observed in comparison to pyrolysis. At the same time, the improvement of hydrocarbon content in pyrolysis oil was contributed by the decomposition of PP. The interaction between PP-derived radicals and carbonyl radicals from OPT contributed to the formation of ketones. A new type of oxygenated compound, alcohols, were formed *via* the intermolecular reactions between PP-derived radicals and hydroxyl radicals from OPT. The findings on the oil composition suggest that the pyrolysis oil is promising as the precursors in the production of value-added biochemicals.

Declaration of Competing Interest

The authors declare that they have no known competing financial interests or personal relationships that could have appeared to influence the work reported in this paper.

Acknowledgements

Liza Melia Terry gratefully acknowledges the Tun Taib Scholarship from Sarawak Foundation. The authors acknowledge the facilities, scientific, and technical support from Advanced Characterization Laboratories Serpong, National Research and Innovation Institute through E-Layanan Sains, Badan Riset and Inovasi National. Also, the authors acknowledge the support for GC–MS analysis from Curtin University,

Malaysia.

Supplementary materials

Supplementary material associated with this article can be found, in the online version, at https://doi.org/10.1016/j.sajce.2022.12.001.

References

Abdullah, N., Sulaiman, F., 2013. The oil palm wastes in Malaysia. In M. D. Matovic (Ed.), Biomass Now - Sustainable Growth and Use: Intechopen.

Abnisa, F., Arami-Niya, A., Wan Daud, W.M.A., Sahu, J.N., Noor, I.M., 2013. Utilization of oil palm tree residues to produce bio-oil and bio-char *via* pyrolysis. Energy Convers. Manag. 76, 1073–1082.

Abnisa, F., Wan Daud, W.M.A., 2014. A review on co-pyrolysis of biomass: an optional technique to obtain a high-grade pyrolysis oil. Energy Convers. Manag. 87, 71–85.

Al-Maari, M.A., Ahmad, M.A., Din, A.T.M., Hassan, H., Alsobaai, A.M., 2021. Co-pyrolysis of oil palm empty fruit bunch and oil palm frond with low-density polyethylene and polypropylene for bio-oil production. Arab. J. Chem. 14, 103282.

ASTM International, 2012. Standard test methods for proximate analysis of coal and coke by macro thermogravimteric analysis. ASTM International, United States.

Brebu, M., Ucar, S., Vasile, C., Yanik, J., 2010. Co-pyrolysis of pine cone with synthetic polymers. Fuel 89, 1911–1918.

Chan, Y.H., Cheah, K.W., How, B.S., Loy, A.C.M., Shahbaz, M., Singh, H.K.G., Yusuf, N.a. R., Shuhaili, A.F.A., Yusup, S., Ghani, W.A.W.A.K., Rambli, J., Kansha, Y., Lam, H.L., Hong, B.H., Ngan, S.L., 2019. An overview of biomass thermochemical conversion technologies in Malaysia. Sci. Total Environ. 680, 105–123.

Charisteidis, I., Lazaridis, P., Fotopoulos, A., Pachatouridou, E., Matsakas, L., Rova, U., Christakopoulos, P., Triantafyllidis, K., 2019. Catalytic fast pyrolysis of lignin isolated by hybrid organosolv—Steam explosion pretreatment of hardwood and softwood biomass for the production of phenolics and aromatics. Catalysts 9, 935.

Chen, H.L., Nath, T.K., Chong, S., Foo, V., Gibbins, C., Lechner, A.M., 2021. The plastic waste problem in Malaysia: Management, recycling and disposal of local and global plastic waste. SN Appl. Sci. 3, 437.

Chin, K.L., Paik San, H.n., Kyin, E., Lee, S.H., Chen, L., Yee, C., 2015. Yield and calorific value of bio oil pyrolysed from oil palm biomass and its relation with solid residence time and process temperature. Asian J. Sci. Res. 8, 351–358.

Deris, R.R.R., Sulaiman, M.R., Darus, F.M., Mahmud, M.S., Bakar, N.A., 2006. Pyrolysis of oil palm trunk (OPT). In: Proceedings of the 20th Symposium of Malaysian Chemical Engineers (SOMChE 2006), pp. 245–250.

Devasahayam, S., Bhaskar Raju, G., Mustansar Hussain, C., 2019. Utilization and recycling of end of life plastics for sustainable and clean industrial processes including the iron and steel industry. Mater. Sci. Energy Technol. 2, 634–646.

Duongbia, N., Kannari, N., Sato, K., Takarada, T., Chaiklangmuang, S., 2022. Production of bio-based chemicals from palmitic acid by catalytic hydrotreating over low-cost Ni/LY char and limonite catalysts. Alex. Eng. J. 61, 3105–3124.

Fukuda, S., 2015. Pyrolysis investigation for bio-oil production from various biomass feedstocks in Thailand. Int. J. Green Energy. 12, 215–224.

Gašparovič, L., Koreňová, Z., Jelemenský, Ľ., 2010. Kinetic study of wood chips decomposition by TGA. Chemical Papers 64, 174–181.

Gonzalez-Garcia, R.A., McCubbin, T., Navone, L., Stowers, C., Nielsen, L.K., Marcellin, E., 2017. Microbial propionic acid production. Fermentation. 3, 21.

Hamzah, N., Tokimatsu, K., Yoshikawa, K., 2019. Solid fuel from oil palm biomass residues and municipal solid waste by hydrothermal treatment for electrical power generation in Malaysia: A review. Sustainability. 11, 1060.

Izzatie, N.I., Basha, M.H., Uemura, Y., Mazlan, M.A., Hashim, M.S.M., Amin, N.A.M., Hamid, M.F., 2016. Co-pyrolysis of rice straw and polypropylene using fixed-bed pyrolyzer. IOP Conf. Ser.: Mater. Sci. Eng. 160, 012033.

Jaya, G.T., Insyani, R., Park, J., Barus, A.F., Sibi, M.G., Ranaware, V., Verma, D., Kim, J., 2022. One-pot conversion of lignocellulosic biomass to ketones and aromatics over a multifunctional Cu–Ru/ZSM-5 catalyst. Appl. Catal. B: Environ. 312, 121368.

Jeon, M.-J., Choi, S., Yoo, K.-S., Ryu, C., Park, S., Lee, J., Jeon, J.-K., Park, Y.-K., Kim, S., 2011. Copyrolysis of block polypropylene with waste wood chip. Korean J. Chem. Eng. 28, 497–501.

Jiang, G., Nowakowski, D.J., Bridgwater, A.V., 2010. Effect of the temperature on the composition of lignin pyrolysis products. Energy Fuels 24, 4470–4475.

Khor, K.H., Lim, K.O., Alimuddin, Z.A.Z., 2010. Laboratory-scale pyrolysis of oil palm trunks. Energy Sources, Part A. 32, 518–531.

Kim, H.-S., Kim, S., Kim, H.-J., Yang, H.-S., 2006. Thermal properties of bio-flour-filled polyolefin composites with different compatibilizing agent type and content. Thermochim. Acta. 451, 181–188.

Kim, J.-Y., Moon, J., Lee, J.H., Jin, X., Choi, J.W., 2020. Conversion of phenol intermediates into aromatic hydrocarbons over various zeolites during lignin pyrolysis. Fuel 279, 118484.

Kohli, K., Prajapati, R., Sharma, B.K., 2019. Bio-based chemicals from renewable biomass for integrated biorefineries. Energies 12, 233.

Kruse, T.M., Wong, H.-W., Broadbelt, L.J., 2003. Mechanistic modeling of polymer pyrolysis: polypropylene. Macromolecules. 36, 9594–9607.

Li, X., Sun, J., Shao, S., Hu, X., Cai, Y., 2021. Aldol condensation/hydrogenation for jet fuel from biomass-derived ketone platform compound in one pot. Fuel Process. Technol. 215, 106768.

Lin, Yu-Chuan, Cho, J., Tompsett, G.A., Westmoreland, P.R., Huber, G.W., 2009. Kinetics and mechanism of cellulose pyrolysis. J. Phys. Chem. C. 113, 20097–20107.

Lin, X., Zhang, Z., Wang, Q., Sun, J., 2020. Interactions between biomass-derived components and polypropylene during wood–plastic composite pyrolysis. Biomass Convers. Biorefin. 3345–3357.

Machado, H., Cristino, A.F., Orišková, S., Galhano dos Santos, R., 2022. Bio-oil: the next-generation source of chemicals. Reactions 3, 118–137.

Mandalika, A., Qin, L., Sato, T.K., Runge, T., 2014. Integrated biorefinery model based on production of furans using open-ended high yield processes. Green Chem 16, 2480–2489.

Mank, V., Polonska, T., 2016. Use of natural oils as bioactive ingredients of cosmetic products. Ukr. Food J. 5, 281–289.

Mohammed, I., Abakr, Y.A., Feroz, K., Suzana, Y., Mohamed Alshareef, I., Chin, S., 2015. Pyrolysis of oil palm residues in a fixed bed tubular reactor. J. Power Energy Eng. 03, 185–193.

Niziolek, A.M., Onel, O., Guzman, Y.A., Floudas, C.A., 2016. Biomass-based production of benzene, toluene, and xylenes *via* methanol: process synthesis and deterministic global optimization. Energy Fuels 30, 4970–4998.

Ojha, D.K., Vinu, R., 2015. Fast co-pyrolysis of cellulose and polypropylene using Py-GC/MS and Py-FT-IR. RSC Adv. 5, 66861–66870.

Palamanit, A., Khongphakdi, P., Tirawanichakul, Y., Phusunti, N., 2019. Investigation of yields and qualities of pyrolysis products obtained from oil palm biomass using an agitated bed pyrolysis reactor. Biofuel Res. J. 6, 1065–1079.

Park, K.-B., Jeong, Y.-S., Kim, J.-S., 2019. Activator-assisted pyrolysis of polypropylene. Appl. Energy 253, 113558.

Parku, G.K., Collard, F.-X., Görgens, J.F., 2020. Pyrolysis of waste polypropylene plastics for energy recovery: Influence of heating rate and vacuum conditions on composition of fuel product. Fuel Process. Technol. 209, 106522.

Prinsen, P., Luque, R., González-Arellano, C., 2018. Zeolite catalyzed palmitic acid esterification. Microporous Mesoporous Mater 262, 133–139.

Rotliwal, Y.C., Parikh, P.A., 2011. Study on thermal co-pyrolysis of Jatropha deoiled cake and polyolefins. Waste Manag. Res. 29, 1251–1261.

Singh, R.K., Ruj, B., Sadhukhan, A.K., Gupta, P., 2019. Thermal degradation of waste plastics under non-sweeping atmosphere: Part 1: Effect of temperature, product optimization, and degradation mechanism. J. Environ. Manage. 239, 395–406.

Sluiter, A., James, B., Ruiz, R., Scarlata, C., Sluiter, J., Templeton, D., Crocker, D., 2012. Determination of structural carbohydrates and lignin in biomass. In: Laboratory analytical procedure (LAP). National Renewable Energy Laboratory (NREL), Midwest Research Institute.

Sluiter, A., Ruiz, R., Scarlata, C., Sluiter, J., Templeton, D., 2005. Determination of extractives in biomass. In: Laboratory analytical procedure (LAP). National Renewable Energy Laboratory (NREL), Midwest Research Institute.

Soh, M., Chew, J., Sunarso, J., 2020. Thermogravimetric analyses (TGA) of three oil palm biomass pyrolysis: Kinetics and reaction mechanisms. IOP Conference Series: Mater. Sci. Eng. 778, 012100.

Stefanidis, S.D., Kalogiannis, K.G., Iliopoulou, E.F., Michailof, C.M., Pilavachi, P.A., Lappas, A.A., 2014. A study of lignocellulosic biomass pyrolysis *via* the pyrolysis of cellulose, hemicellulose and lignin. J. Anal. Appl. Pyrolysis. 105, 143–150.

Sukiran, M., Loh, S.K., Abu Bakar, N., 2016. Production of bio-oil from fast pyrolysis of oil palm biomass using fluidised bed reactor. J. Energy Tech. Pol. 6, 52–62.

Suriapparao, D.V., Yerrayya, A., Nagababu, G., Guduru, R.K., Kumar, T.H., 2020. Recovery of renewable aromatic and aliphatic hydrocarbon resources from microwave pyrolysis/co-pyrolysis of agro-residues and plastics wastes. Bioresour. Technol. 318, 124277.

TAPPI, 2006. Acid-insoluble lignin in wood and pulp (Reaffirmation of T 222 om-02). TAPPI, Georgia, US.

Usino, D.O., Supriyanto Ylitervo, P., Pettersson, A., Richards, T., 2020. Influence of temperature and time on initial pyrolysis of cellulose and xylan. J. Anal. Appl. Pyrolysis. 147, 104782.

Wang, S.-R., Liang, T., Ru, B., Guo, X.-J., 2013. Mechanism of xylan pyrolysis by Py-GC/MS. Chem. Res. Chin. Univ. 29, 782–787.

Wu, F., Ben, H., Yang, Y., Jia, H., Wang, R., Han, G., 2020. Effects of different conditions on co-pyrolysis behavior of corn Stover and polypropylene. Polymers (Basel) 12, 973.

Xue, J., Zhuo, J., Liu, M., Chi, Y., Zhang, D., Yao, Q., 2017. Synergetic effect of co-pyrolysis of cellulose and polypropylene over an all-silica mesoporous catalyst MCM-41 using thermogravimetry–fourier transform infrared spectroscopy and pyrolysis–gas chromatography–mass spectrometry. Energy Fuels 31, 9576–9584.

Yaman, S., 2004. Pyrolysis of biomass to produce fuels and chemical feedstocks. Energy Convers. Manag. 45, 651–671.

Yang, H., Yan, R., Chen, H., Zheng, C., Lee, D.H., Liang, D.T., 2006. In-depth investigation of biomass pyrolysis based on three major components: Hemicellulose, cellulose and lignin. Energy Fuels 20, 388–393.

Zhang, X., Lei, H., Chen, S., Wu, J., 2016. Catalytic co-pyrolysis of lignocellulosic biomass with polymers: A critical review. Green Chem. 18, 4145–4169.

Zhang, X., Qiao, P., Ji, X., Han, J., Liu, L., Weeks, B.L., Yao, Q., Zhang, Z., 2013. Sustainable recycling of benzoic acid production waste: green and highly efficient methods to separate and recover high value-added conjugated aromatic compounds from industrial residues. ACS Sustain. Chem. Eng. 1, 974–981.

Zhao, C., Jiang, E., Chen, A., 2017. Volatile production from pyrolysis of cellulose, hemicellulose and lignin. J. Energy Inst. 90, 902–913.